

The Second Order Linear Model

Ming Lin^{*1}, Shuang Qiu^{†1}, Bin Hong^{‡2} and Jieping Ye^{§1}

¹Department of Computational Medicine and Bioinformatic,
University of Michigan, Ann Arbor, MI 48109

²State Key Lab of CAD&G, Zhejiang University, Hangzhou,
China, 310058

May 7, 2022

Abstract

The second order linear model (SLM) extends the linear model to high order functional space. Special cases of the SLM have been widely studied under various restricted assumptions during the past decade. Yet how to efficiently learn the SLM under full generality still remains an open question due to several fundamental limitations of the conventional gradient descent learning framework. In this introductory study, we try to attack this problem from a gradient-free approach which we call the moment-estimation-sequence (MES) method. We show that the conventional gradient descent heuristic is biased by the skewness of the distribution therefore is no longer the best practice of learning the SLM. Based on the MES framework, we design a nonconvex alternating iteration process to train a d -dimension rank- k SLM within $O(kd)$ memory and one-pass of the dataset. The proposed method converges globally and linearly, achieves ϵ recovery error after retrieving $O[k^2d \cdot \text{polylog}(kd/\epsilon)]$ samples. Furthermore, our theoretical analysis reveals that not all SLMs can be learned on every sub-gaussian distribution. When the instances are sampled from a so-called τ -MIP distribution, the SLM can be learned by $O(p/\tau^2)$ samples where p and τ are positive constants depending on the skewness and kurtosis of the distribution. For non-MIP distribution, an addition diagonal-free oracle is necessary and sufficient to guarantee the learnability of the SLM. Numerical simulations verify the sharpness of our bounds on the sampling complexity and the linear convergence rate of our algorithm. Finally we demonstrate several applications of the SLM on large-scale high dimensional datasets.

^{*}linmin@umich.edu

[†]qiush@umich.edu

[‡]bin_hong@zju.edu.cn

[§]jpye@umich.edu

1 Introduction

Linear model plays a key role in contemporary machine learning due to its great success in real-world problems and nice theoretical properties Koltchinskii [2011]. An obvious limitation of the linear model is its incompetence of modeling the non-linear relationship. In order to apply the linear model to non-linear problems, a vast amount of extensions have been studied in the past decades, such as the kernel trick [Hofmann et al., 2008] or the explicit feature mapping [Vedaldi and Zisserman, 2012]. These extensions have their own advantages and disadvantages and are still under active research.

In this work we introduce a straightforward extension of the linear model to the second order functional space which we call the *second order linear model* (SLM). Considering an SLM parameterized by the first order coefficient $\mathbf{w}^* \in \mathbb{R}^d$ and the second order coefficient $M^* \in \mathbb{R}^{d \times d}$. Given an instance $\mathbf{x} \in \mathbb{R}^d$ randomly sampled from coordinate sub-gaussian distribution, its label $y \in \mathbb{R}$ is assumed to be generated from

$$y = \mathbf{x}^\top \mathbf{w}^* + \mathbf{x}^\top M^* \mathbf{x} + \xi \quad (1)$$

where ξ is an additive sub-gaussian noise term. The SLM defined in Eq. (1) generalizes several important models in machine learning and signal processing. When $\mathbf{w}^* = 0$ and M^* is a rank-one symmetric matrix, Eq. (1) is known as the phase retrieval problem [Candes et al., 2013]. While M^* is a rank- k symmetric matrix, Eq. (1) is equal to the symmetric rank-one matrix sensing problem [Kueng et al., 2017, Cai and Zhang, 2015]. For $\mathbf{w}^* \neq \mathbf{0}$ and $M_{i,j}^* = v_i v_j$ at $i \neq j$ otherwise $M_{i,i}^* = 0$, Eq. (1) is called the Factorization Machine (FM) [Rendle, 2010]. M^* can be any low-rank symmetric matrix when \mathbf{x} is sampled from the Gaussian distribution and the model is called the Generalized Factorization Machine (gFM) [Ming Lin and Jieping Ye, 2016]. It is possible to further extend the SLM to high order functional space which leads to the Polynomial Network model [Blondel et al., 2016]. We will focus on the second order model in this work due to its simplicity. High order linear models will be considered in future work.

Although the above special cases of SLM have been studied under various circumstances, there is rare research of SLM under a general setting in form of Eq. (1). A naive analysis directly following the sampling complexity of the linear model would suggest $O(d^2)$ samples in order to learn the SLM. For high dimensional problems this is too expensive to be useful. We need a more efficient solution with sampling complexity much less than $O(d^2)$, especially when M^* is low-rank. This seemingly simple problem is still an open question by the time of writing this paper. In this introductory work, we try to attack this problem from a nonconvex gradient-free approach which we call the moment-estimation-sequence method. The method is based on nonconvex alternating iteration in one-pass of the data stream within $O(kd)$ memory. The proposed method converges globally and linearly. It achieves ϵ recovery error after retrieving $O[k^2 dp/\tau^2 \cdot \text{polylog}(kd/\epsilon)]$ samples where p is a constant depending on the skewness and kurtosis of the distribution and τ is the Moment Invertible

Property (MIP) constant (see Definition 1). When the instance distribution is not τ -MIP, our theoretical analysis reveals that an addition diagonal-free oracle of M^* is necessary and sufficient to guarantee the recovery of the SLM.

There are several fundamental challenges of learning the SLM. Indeed, even the symmetric rank-one matrix sensing problem, a special case of the SLM, is proven to be hard. Until very recently, Cai and Zhang [2015] partially answered the sampling complexity of this special case on well-bounded sub-gaussian distribution using trace norm convex programming under the ℓ_2/ℓ_1 -RIP condition. It is still unclear how to solve this special case using more efficient alternating iteration on general sub-gaussian distribution such as the Bernoulli distribution. Perhaps the most state-of-the-art research on the SLM is the preliminary work by Ming Lin and Jieping Ye [2016]. Their result is still weak because they rely on the rotation invariance of the Gaussian distribution therefore their analysis cannot be generalized to non-Gaussian distributions. Their sampling complexity is $O(k^3d)$ which is suboptimal compared to our $O(k^2d)$ bound. The readers familiar with convex geometry might recall the general convex programming method for structured signal recovery developed by Tropp [2015]. It is difficult to apply Tropp's method here because it is unclear how to lower-bound the conic singular value on the decent cone of the SLM. Our conjecture is that this value is very likely to be zero since Tropp's formulation doesn't consider the MIP condition which is critical in our sampling complexity analysis. Even this value is strictly above zero, we still need to solve a convex conic programming that is less efficient than alternating iteration. We would like to refer the above papers for more historical developments on the related research topics.

The most remarkable trait of our approach is its gradient-free nature. In nonconvex optimization, the gradient descent heuristic usually works well. For most conventional (first order) matrix estimation problems, the gradient descent heuristic happens to be provable Zhao et al. [2015]. In our language, the gradient iteration on these first order problems happens to form a moment estimation sequence. When training the SLM on skewed sub-gaussian distributions, the gradient descent heuristic no longer generates such sequence. The gradient of the SLM will be biased by the skewness of the distribution which can even dominate the gradient norm. This bias must be eliminated which motivates our moment-estimation-sequence construction. Please see subsection 2.1 for an in-depth discussion.

The remainder of this paper is organized as following. In Section 2 we introduce necessary notation and background of the SLM. Subsection 2.1 is devoted to the gradient-free learning principle and the MIP condition. We propose the moment-estimation-sequence method in Section 3. Theorem 2 bounds the convergence rate of our main Algorithm 1. A sketched theoretical analysis is briefed in Section 4. Our key theoretical result is Theorem 5 which is the counterpart of sub-gaussian Hanson-Wright inequality [Rudelson and Vershynin, 2013] on low-rank matrix manifold. Section 5 conducts numerical simulations to verify our analysis followed by several demonstrative applications of the SLM in large-scale high dimensional problems. Section 6 concludes this work.

2 Notation and Background

Suppose we are given n training instances $\mathbf{x}^{(i)}$ for $i \in \{1, \dots, n\}$ and the corresponding labels y_i identically and independently (i.i.d.) sampled from a joint distribution $P(\mathbf{x}, y)$. Denote the feature matrix $X = [\mathbf{x}^{(1)}, \dots, \mathbf{x}^{(n)}] \in \mathbb{R}^{d \times n}$ and the label vector $\mathbf{y} = [y_1, \dots, y_n]^\top \in \mathbb{R}^n$. The SLM defined in Eq. (1) can be written in the matrix form

$$\mathbf{y} = X^\top \mathbf{w}^* + \mathcal{A}(M^*) + \boldsymbol{\xi} \quad (2)$$

where the operator $\mathcal{A}(\cdot) : \mathbb{R}^{d \times d} \rightarrow \mathbb{R}^d$ is defined by

$$\mathcal{A}(M) \triangleq [\mathbf{x}^{(1)\top} M \mathbf{x}^{(1)}, \dots, \mathbf{x}^{(n)\top} M \mathbf{x}^{(n)}] . \quad (3)$$

The operator \mathcal{A} is called the rank-one symmetric matrix sensing operator since $\mathbf{x}^\top M \mathbf{x} = \langle \mathbf{x} \mathbf{x}^\top, M \rangle$ where the sensing matrix $\mathbf{x} \mathbf{x}^\top$ is of rank-one and symmetric. The adjoint operator of \mathcal{A} is \mathcal{A}' . To make the learning problem well-defined, it is necessary to assume M^* to be a symmetric low-rank matrix Ming Lin and Jieping Ye [2016]. We assume \mathbf{x} is coordinate sub-gaussian with mean zero and unit variance. The elementwise third order moment of \mathbf{x} is denoted as $\boldsymbol{\kappa}^* \triangleq \mathbb{E} \mathbf{x}^3$ and the fourth order moment is $\boldsymbol{\phi}^* \triangleq \mathbb{E} \mathbf{x}^4$. For sub-gaussian random variable z , we denote its ψ_2 -Orlicz norm Koltchinskii [2011] as $\|z\|_{\psi_2}$. Without loss of generality we assume each coordinate of \mathbf{x} is bounded by unit sub-gaussian norm, that is, $\|\mathbf{x}_i\|_{\psi_2} \leq 1$ for $i \in \{1, \dots, d\}$. The matrix Frobenius norm, nuclear norm and spectral norm are denoted as $\|\cdot\|_F$, $\|\cdot\|_*$, $\|\cdot\|_2$ respectively. We use I to denote identity matrix or identity operator whose dimension or domain can be inferred from context. $\mathcal{D}(\cdot)$ denotes the diagonal function. For any two matrices A and B , we denote their Hadamard product as $A \circ B$. The elementwise squared matrix is defined by $A^2 \triangleq A \circ A$. For a non-negative real number $\xi \geq 0$, the symbol $O(\xi)$ denotes some perturbation matrix whose spectral norm is upper bounded by ξ . The i -th largest singular value of matrix M is $\sigma_i(M)$. To abbreviate our high probability bounds, given a probability η , we use symbol C_η and c_η to denote some factors polynomial logarithmic in $1/\eta$ and any other necessary variables that do not change the polynomial order of our bounds.

Estimating $\{\mathbf{w}^*, M^*\}$ with $n \ll O(d^2)$ is an ill-posed problem without additional structure knowledge about M^* . In matrix sensing literatures, the most popular assumption is that M^* is low-rank. Following the standard convex relaxation, we could penalize the rank of M approximately by nuclear norm which leads to the convex optimization problem

$$\min_{\mathbf{w}, M} \frac{1}{2n} \|X^\top \mathbf{w} + \mathcal{A}(M) - \mathbf{y}\|^2 + \frac{\lambda}{n} \|M\|_* . \quad (4)$$

Although the state-of-the-art nuclear norm solvers can handle large scale problems when the feature is sparse, minimizing Eq. (4) is still computationally expensive. An alternative more efficient approach is to decompose M as product of two low-rank matrices $M = UV^\top$ where $U, V \in \mathbb{R}^{d \times k}$. To this end we

turn to a nonconvex optimization problem:

$$\min_{\mathbf{w}, U, V} \mathcal{L}(\mathbf{w}, U, V) \triangleq \frac{1}{2n} \|X^\top \mathbf{w} + \mathcal{A}(UV^\top) - \mathbf{y}\|^2. \quad (5)$$

Heuristically, one can solve Eq. (5) by updating \mathbf{w}, U, V via alternating gradient descent. Due to the nonconvexity, it is challenging to derive the global convergent guarantee for this kind of heuristic algorithms. If the problem is simple enough, such as the asymmetric matrix sensing problem, the heuristic alternating gradient descent might work well. However, in our problem this is no longer true. Naive gradient descent will lead to non-convergent behavior due to the symmetric matrix sensing. To design a global convergent nonconvex algorithm, we need a novel gradient-free learning framework which we call the moment-estimation-sequence method. We will present the high level idea of this technique in subsection 2.1.

2.1 Learning without Gradient Descent

In this subsection, we will discuss several fundamental challenges of learning the SLM. We will show that the conventional gradient descent is no longer a good heuristic. This motivates us looking for a gradient-free approach which leads to the moment-estimation-sequence method.

To see why gradient descent is a bad idea, let us compute the expected gradient of $\mathcal{L}(\mathbf{w}^{(t)}, U^{(t)}, V^{(t)})$ with respect to $V^{(t)}$ at step t .

$$\begin{aligned} & \mathbb{E} \nabla_V \mathcal{L}(\mathbf{w}^{(t)}, U^{(t)}, V^{(t)}) \\ &= \mathbb{E} \frac{1}{n} \mathcal{A}' [X^\top \mathbf{w}^{(t)} + \mathcal{A}(U^{(t)} V^{(t)\top}) - \mathbf{y}] U^{(t)} \\ &= 2(M^{(t)} - M^*) U^{(t)} + F^{(t)} U^{(t)} \end{aligned} \quad (6)$$

where

$$\begin{aligned} F^{(t)} &= \text{tr}(M^{(t)} - M^*) I + \mathcal{D}(\phi - 3) \mathcal{D}(M^{(t)} - M^*) \\ &\quad + \mathcal{D}(\kappa) \mathcal{D}(\mathbf{w}^{(t)} - \mathbf{w}^*). \end{aligned}$$

In previous nonconvex problems, we expect $\mathbb{E} \nabla \mathcal{L} \approx I$ in order to establish the global convergence rate. However this is no longer the case in our problem. From Eq. (6), $\|\frac{1}{2} \mathbb{E} \nabla \mathcal{L} - I\|_2$ is dominated by $\|\kappa\|_\infty$ and $\|\phi - 3\|_\infty$. For non-Gaussian distributions, these two perturbation terms can be easily large enough to prevent the global convergence of the algorithm. The divergence not only appears in the theoretical analysis but also is observable in numerical experiments. Please check our experiment section for simulation results of gradient descent algorithm with divergent behavior. The gradient of \mathbf{w} is similarly biased by $O(\|\kappa\|_\infty)$.

The failure of gradient descent inspires us looking for a gradient-free learning method. The perturbation terms in Eq. (6) are high order moments of sub-gaussian variable \mathbf{x} . It might be possible to construction a sequence of high order moments to eliminate these perturbation terms. We call this idea the

moment-estimation-sequence method. In the proposed method, we do not try to minimize the empirical loss. Instead, our global convergence rate is established via Nesterov’s estimation sequence argument Nesterov [2004].

The next critical question is whether the desired moment estimation sequence exists and how to construct it efficiently. Unfortunately, specific to the SLM on sub-gaussian distribution, this is impossible in general. We need an addition but mild enough assumption on the sub-gaussian distribution which we call the *Moment Invertible Property* (MIP).

Definition 1 (Moment Invertible Property). A sub-gaussian distribution is called τ -Moment Invertible if $|\phi - 1 - \kappa^2| \geq \tau$ for some constant $\tau > 0$.

The definition of τ -MIP is motivated by our estimation sequence construction. When the MIP cannot be satisfied, one cannot eliminate the perturbation terms via the moment-estimation-sequence method and no global convergence rate to M^* can be guaranteed. An exemplar distribution doesn’t satisfy the MIP is the Bernoulli distribution. In order to learn the SLM on non-MIP distributions, we need to further assume M^* to be diagonal-free. That is, $M^* = \bar{M}^* - \mathcal{D}(\bar{M}^*)$ where \bar{M}^* is low-rank and symmetric. It is interesting to note that M^* in this case is actually full-rank but still recoverable since we have the knowledge about its low-rank structure \bar{M}^* .

3 The Moment-Estimation-Sequence Method

In this section, we construct the moment estimation sequence for MIP distribution in Algorithm 1 and non-MIP distribution in subsection 3.1. We will focus on the high level intuition of our construction in this section. The theoretical analysis is given in Section 4.

Suppose \mathbf{x} is i.i.d. sampled from a MIP distribution. Our moment estimation sequence is constructed in Algorithm 1. Denote $\{\mathbf{w}^{(t)}, M^{(t)}\}$ to be an estimation sequence of $\{\mathbf{w}^*, M^*\}$ where $M^{(t)} = U^{(t)}V^{(t)\top}$. We will show that $\|\mathbf{w}^{(t)} - \mathbf{w}^*\|_2 + \|M^{(t)} - M^*\|_2 \rightarrow 0$ as $t \rightarrow \infty$. The key idea of our construction is to eliminate $F^{(t)}$ in the expected gradient. By construction,

$$\begin{aligned} \mathcal{P}^{(t,0)}(\hat{\mathbf{y}}^{(t)} - \mathbf{y}^{(t)}) &\approx \text{tr}(M^{(t)} - M^*) \\ \mathcal{P}^{(t,1)}(\hat{\mathbf{y}}^{(t)} - \mathbf{y}^{(t)}) &\approx D(M^{(t)} - M^*)\kappa + \mathbf{w}^{(t)} - \mathbf{w}^* \\ \mathcal{P}^{(t,2)}(\hat{\mathbf{y}}^{(t)} - \mathbf{y}^{(t)}) &\approx D(M^{(t)} - M^*)(\phi - 1) \\ &\quad + D(\kappa)(\mathbf{w}^{(t)} - \mathbf{w}^*) . \end{aligned}$$

This inspires us to find a linear combination of $\mathcal{P}^{(t,\cdot)}$ to eliminate $F^{(t)}$ which leads to the linear equations Eq. (7). Namely, we want to construct $\{\mathcal{M}^{(t)}, \mathcal{W}^{(t)}\}$ such that $\mathcal{M}^{(t)}(\hat{\mathbf{y}}^{(t)} - \mathbf{y}^{(t)}) \approx M^{(t)} - M^*$ and $\mathcal{W}^{(t)}(\hat{\mathbf{y}}^{(t)} - \mathbf{y}^{(t)}) \approx \mathbf{w}^{(t)} - \mathbf{w}^*$. The rows of G are exactly the coefficients of $\mathcal{P}^{(t,\cdot)}$ we are looking for to construct $\mathcal{M}^{(t)}$. We construct $\mathcal{W}^{(t)}$ similarly by solving Eq. (8). In Eq. (7) and (8), the matrix inversion is numerically stable if and only if the distribution of \mathbf{x}

Algorithm 1 Moment Estimation Sequence Method

Require: The mini-batch size n ; number of total update T ; training instances $X^{(t)} \triangleq [\mathbf{x}^{(t,1)}, \mathbf{x}^{(t,2)}, \dots, \mathbf{x}^{(t,n)}]$, $\mathbf{y}^{(t)} \triangleq [y^{(t,1)}, y^{(t,2)}, \dots, y^{(t,n)}]^\top$; rank $k \geq 1$

Ensure: $\mathbf{w}^{(T)}, U^{(T)}, V^{(T)}, M^{(t)} \triangleq U^{(t)}V^{(t)\top}$.

1: For any $\mathbf{z} \in \mathbb{R}^n$ and $M \in \mathbb{R}^{d \times d}$, define function

$$\begin{aligned}\mathcal{P}^{(t,0)}(\mathbf{z}) &\triangleq \mathbf{1}^\top \mathbf{z}/n, \quad \mathcal{P}^{(t,1)}(\mathbf{z}) \triangleq X^{(t)} \mathbf{z}/n \\ \mathcal{P}^{(t,2)}(\mathbf{z}) &\triangleq (X^{(t)})^2 \mathbf{z}/n - \mathcal{P}^{(t,0)}(\mathbf{z}) \\ \mathcal{A}^{(t)}(M) &\triangleq \mathcal{D}(X^{(t)\top} M X^{(t)}) \\ \mathcal{H}^{(t)}(\mathbf{z}) &\triangleq \mathcal{A}^{(t)'} \mathcal{A}^{(t)}(\mathbf{z})/(2n).\end{aligned}$$

2: Retrieve n training instances to estimate the third and fourth order moments κ and ϕ .
3: For $j \in \{1, \dots, d\}$, solve $G \in \mathbb{R}^{d \times 2}$ and $H \in \mathbb{R}^{d \times 2}$ where the j -th row of G and H are

$$G_{i,:}^\top = \begin{bmatrix} 1 & \kappa_j \\ \kappa_j & \phi_j - 1 \end{bmatrix}^{-1} \begin{bmatrix} \kappa_j \\ \phi_j - 3 \end{bmatrix}. \quad (7)$$

$$H_{i,:}^\top = \begin{bmatrix} 1 & \kappa_j \\ \kappa_j & \phi_j - 1 \end{bmatrix}^{-1} \begin{bmatrix} 1 \\ 0 \end{bmatrix}. \quad (8)$$

4: Initialize: $\mathbf{w}^{(0)} = \mathbf{0}$, $V^{(0)} = 0$. $U^{(0)} = \text{SVD}(\mathcal{H}^{(0)}(\mathbf{y}^{(0)}), k)$, that is, the top- k left singular vector.
5: **for** $t = 1, 2, \dots, T$ **do**
6: Retrieve n training instances $X^{(t)}, \mathbf{y}^{(t)}$.
7: Compute

$$\begin{aligned}\hat{\mathbf{y}}^{(t)} &= X^{(t)\top} \mathbf{w}^{(t-1)} + \mathcal{A}^{(t)}(U^{(t-1)} V^{(t-1)\top}) \\ \mathcal{M}^{(t)}(\hat{\mathbf{y}}^{(t)} - \mathbf{y}^{(t)}) &\triangleq \mathcal{H}^{(t)}(\hat{\mathbf{y}}^{(t)} - \mathbf{y}^{(t)}) \\ &\quad - \frac{1}{2} \mathcal{D} \left(G_1 \circ \mathcal{P}^{(t,1)}(\hat{\mathbf{y}}^{(t)} - \mathbf{y}^{(t)}) \right) \\ &\quad - \frac{1}{2} \mathcal{D} \left(G_2 \circ \mathcal{P}^{(t,2)}(\hat{\mathbf{y}}^{(t)} - \mathbf{y}^{(t)}) \right) \\ \hat{U}^{(t)} &= V^{(t-1)} - \mathcal{M}^{(t)}(\hat{\mathbf{y}}^{(t)} - \mathbf{y}^{(t)}) U^{(t-1)}\end{aligned}$$

8: Orthogonalize $\hat{U}^{(t)}$ via QR decomposition: $U^{(t)} R^{(t)} = \hat{U}^{(t)}$.
9: $V^{(t)} = V^{(t-1)} R^{(t)\top}$.
10: $\mathcal{W}^{(t)}(\hat{\mathbf{y}}^{(t)} - \mathbf{y}^{(t)}) \triangleq H_1 \circ \mathcal{P}^{(t,1)}(\hat{\mathbf{y}}^{(t)} - \mathbf{y}^{(t)}) + H_2 \circ \mathcal{P}^{(t,2)}(\hat{\mathbf{y}}^{(t)} - \mathbf{y}^{(t)})$.
11: $\mathbf{w}^{(t)} = \mathbf{w}^{(t-1)} - \mathcal{W}^{(t)}(\hat{\mathbf{y}}^{(t)} - \mathbf{y}^{(t)})$.
12: **end for**
13: **Output:** $\mathbf{w}^{(T)}, U^{(T)}, V^{(T)}$.

is τ -MIP. For non-MIP distributions, Eq. (7) is singular therefore we couldn't eliminate the gradient bias in this case. Please see subsection 3.1 for an alternative solution on non-MIP distribution.

The following theorem gives the global convergence rate of Algorithm 1 under noise-free condition.

Theorem 2. *In Algorithm 1, suppose $\{\mathbf{x}^{(t,i)}, y^{(t,i)}\}$ are i.i.d. sampled from model (1). The vector $\mathbf{x}^{(t,i)}$ is coordinate sub-gaussian of mean zero and unit variance. Each dimension of $\mathbb{P}(\mathbf{x})$ is τ -MIP. The noise term $\boldsymbol{\xi} = \mathbf{0}$ and M^* is a rank- k matrix. Then with probability at least $1 - \eta$,*

$$\|\mathbf{w}^{(t)} - \mathbf{w}^*\|_2 + \|M^{(t)} - M^*\|_2 \leq \delta^t (\|\mathbf{w}^*\|_2 + \|M^*\|_2) ,$$

provided $n \geq C_\eta(p+1)^2/\delta^2 \max\{p/\tau^2, k^2d\}$ and

$$\delta \leq \frac{(4\sqrt{5}\sigma_1^*/\sigma_k^* + 3)\sigma_k^*}{4\sqrt{5}\sigma_1^* + 3\sigma_k^* + 4\sqrt{5}\|\mathbf{w}^*\|_2^2} , \quad (9)$$

where $p \triangleq \max\{1, \|\boldsymbol{\kappa}^*\|_\infty, \|\boldsymbol{\phi}^* - 3\|_\infty, \|\boldsymbol{\phi}^* - 1\|_\infty\}$.

In Theorem 2, we measure the quality of our estimation by the recovery error $\|\mathbf{w}^{(t)} - \mathbf{w}^*\|_2 + \|M^{(t)} - M^*\|_2$ at step t . Choosing a small enough number δ , Algorithm 1 converges linearly with rate δ . A small δ will require a large $n \approx O(1/\delta^2)$. Equivalently speaking, when n is larger than the required sampling complexity, the convergence rate is around $\delta^t \approx O(n^{-t/2})$. The sampling complexity is on order of $\max\{O(k^2d), O(1/\tau^2)\}$. For the Gaussian distribution $\tau = 2$ therefore the sampling complexity is $O(k^2d)$ for nearly Gaussian distribution. When τ is small, $\mathbb{P}(\mathbf{x})$ is nearly non-MIP therefore we need the non-MIP construction of the moment estimation sequence which is presented in subsection 3.1.

Theorem 2 only considers the noise-free case. The noisy result is similar to Theorem 2 under the small noise condition [Ming Lin and Jieping Ye, 2016]. Roughly speaking, our estimation will linearly converge to the statistical error level if the noise is small and M^* is nearly low-rank. We will leave the noisy case to the journal version of this work.

3.1 Non-MIP Distribution

For non-MIP distributions, it is no longer possible to construct the moment estimation sequence in the same way as MIP distributions because Eq. (7) will be singular. The essential difficulty is due to the $\mathcal{D}(M^*)$ related bias terms in the gradient. Therefore for non-MIP distributions, it is necessary to assume M^* to be diagonal-free, that is, $\mathcal{D}(M^*) = \mathcal{D}(\mathbf{0})$. More specifically, we assume that \bar{M}^* is a low-rank matrix and $M^* = \bar{M}^* - \mathcal{D}(\bar{M}^*)$. Please note that M^* might be a full-rank matrix now.

We follow the construction in Algorithm 1. We replace $M^{(t)}$ in Algorithm 1 with $M^{(t)} = U^{(t)}V^{(t)\top} - \mathcal{D}(U^{(t)}V^{(t)\top})$. Since $\mathcal{D}(M^{(t)} - M^*) = \mathcal{D}(\mathbf{0})$, denote

$$\begin{aligned}
\mathbf{z}^{(t)} &\triangleq \hat{\mathbf{y}}^{(t)} - \mathbf{y}^{(t)}, \\
\mathcal{P}^{(t,1)}(\mathbf{z}^{(t)}) &\approx \mathbf{w}^{(t)} - \mathbf{w}^* \\
\mathcal{P}^{(t,2)}(\mathbf{z}^{(t)}) &\approx D(\boldsymbol{\kappa})(\mathbf{w}^{(t)} - \mathbf{w}^*) \\
\mathcal{H}^{(t)}(\mathbf{z}^{(t)}) &\approx (M^{(t)} - M^*) + \mathcal{D}(\boldsymbol{\kappa})\mathcal{D}(\mathbf{w}^{(t)} - \mathbf{w}^*)/2 .
\end{aligned}$$

Therefore, we can construct our moment estimation sequence as following:

$$\begin{aligned}
\mathcal{M}^{(t)}(\mathbf{z}^{(t)}) &= \mathcal{H}^{(t)}(\mathbf{z}^{(t)}) - \mathcal{D}[\mathcal{P}^{(t,2)}(\mathbf{z}^{(t)})/2] \\
\mathcal{W}^{(t)}(\mathbf{z}^{(t)}) &= \mathcal{P}^{(t,1)}(\mathbf{z}^{(t)}) .
\end{aligned}$$

The rest part is the same as Algorithm 1.

4 Theoretical Analysis

In this section, we present the proof sketch of Theorem 2. Details are postponed to the appendix. Define

$$\beta_t \triangleq \|\mathbf{w}^{(t)} - \mathbf{w}^*\|_2, \quad \gamma_t \triangleq \|M^{(t)} - M^*\|_2, \quad \epsilon_t \triangleq \beta_t + \gamma_t .$$

Our essential idea is to construct

$$\begin{aligned}
\mathcal{M}^{(t)}(\hat{\mathbf{y}}^{(t)} - \mathbf{y}^{(t)}) &= M^{(t-1)} - M^* + O(\delta\epsilon_{t-1}) \\
\mathcal{W}^{(t)}(\hat{\mathbf{y}}^{(t)} - \mathbf{y}^{(t)}) &= \mathbf{w}^{(t-1)} - \mathbf{w}^* + O(\delta\epsilon_{t-1}) .
\end{aligned} \tag{10}$$

for some small $\delta \geq 0$. Once we have constructed Eq. (10), we can apply the noisy power iteration analysis as in [Ming Lin and Jieping Ye, 2016]. The global convergence rate immediately follows from Theorem 3 given below.

Theorem 3 (Theorem 1 in [Ming Lin and Jieping Ye, 2016]). *Suppose $\{M^{(t)}, \mathbf{w}^{(t)}\}$ constructed in Algorithm 1 satisfy Eq. (10). The noisy term $\boldsymbol{\xi} = 0$ and M^* is of rank k . Then after t iteration,*

$$\|\mathbf{w}^{(t)} - \mathbf{w}^*\|_2 + \|M^{(t)} - M^*\|_2 \leq \delta^t (\|\mathbf{w}^*\|_2 + \|M^*\|_2) ,$$

provided δ satisfying Eq. (9) .

Theorem 3 shows that the recovery error of the sequence $\{\mathbf{w}^{(t)}, M^{(t)}\}$ will converges linearly with rate δ as long as Eq. (10) holds true. The next question is whether Eq. (10) can be satisfied with a small δ . To answer this question, we will show that $\mathcal{M}^{(t)}$ and $\mathcal{W}^{(t)}$ are nearly isometric operators with no more than $O(C_\eta k^2 d)$ samples.

In low-rank matrix sensing, the Restricted Isometric Property (RIP) of sensing operator \mathcal{A} determinates the sampling complexity of recovery. However in the SLM, \mathcal{A} is a symmetric rank-one sensing operator therefore the conventional RIP condition is too strong to hold true. Following Ming Lin and Jieping Ye [2016], we introduce a weaker requirement, the Conditionally Independent RIP (CI-RIP) condition.

Definition 4 (CI-RIP). Suppose $k \geq 1$, $\delta_k > 0$, M is a fixed rank k matrix. A sensing operator \mathcal{A} is called δ_k CI-RIP if for a fixed M , \mathcal{A} is sampled independently such that

$$(1 - \delta_k) \|M\|_F^2 \leq \|\mathcal{A}(M)\|_2^2 \leq (1 + \delta_k) \|M\|_F^2.$$

Comparing to the conventional RIP condition, the CI-RIP only requires the isometric property to hold on a fixed low-rank matrix rather than any low-rank matrix. The corresponding price is that \mathcal{A} should be independently sampled from $M^{(t)}$. This can be achieved by resampling at each iteration. Since our algorithm converges linearly, the resampling takes logarithmically more samples therefore it will not affect the order of sampling complexity.

The CI-RIP defined in Definition 4 concerns about the concentration of \mathcal{A} around zero. The next theorem shows that \mathcal{A} in the SLM concentrates around its expectation. That is, \mathcal{A} is CI-RIP after shifted by its expectation. The proof can be found in Appendix B.

Theorem 5 (Sub-gaussian shifted CI-RIP). *Under the same settings of Theorem 2, suppose $d \geq 2(\sqrt{k} + 2 + \|\phi^* - 3\|_\infty)$. Fixed a rank k matrix M , with probability at least $1 - \eta$, provided $n \geq C_\eta kd/\delta^2$,*

$$\begin{aligned} \frac{1}{n} \mathcal{A}' \mathcal{A}(M) &= 2M + \text{tr}(M)I + \mathcal{D}(\phi^* - 3)\mathcal{D}(M) \\ &\quad + O(\delta\|M\|_2). \end{aligned}$$

Theorem 5 is one of the main contributions of this work. Comparing to previous results, mostly Theorem 4 in [Ming Lin and Jieping Ye, 2016], we have several fundamental improvements. First it allows sub-gaussian distribution which requires a more challenging analysis. Secondly, the sampling complexity is $O(C_\eta k^2 d)$ which is better than previous $O(C_\eta k^3 d)$ bounds. Recall that the information-theoretical low bound requires at least $O(C_\eta kd)$ complexity. Therefore our bound is slightly $O(k)$ worse than the best possible bound. The key ingredient of our proof is a fixed-point concentration followed by low-rank covering net argument [Candes and Plan, 2011], together with sub-gaussian Hanson-Wright inequality provided in [Rudelson and Vershynin, 2013]. Please check Appendix B for more details.

Based on the shifted CI-RIP condition of operator \mathcal{A} , it is straightforward to prove the following perturbation bounds.

Lemma 6. *Under the same settings of Theorem 2, with probability at least $1 - \eta$, for fixed $\mathbf{y} = X^\top \mathbf{w} + \mathcal{A}(M)$,*

$$\begin{aligned} \frac{1}{n} \mathcal{A}'(X^\top \mathbf{w}) &= \mathcal{D}(\kappa^*)\mathbf{w} + O(\delta\|\mathbf{w}\|_2) \\ \mathcal{P}^{(0)}(\mathbf{y}) &\triangleq \frac{1}{n} \mathbf{1}^\top \mathbf{y} = \text{tr}(M) + O[\delta(\|\mathbf{w}\|_2 + \|M\|_2)] \\ \mathcal{P}^{(1)}(\mathbf{y}) &\triangleq \frac{1}{n} X \mathbf{y} = \mathcal{D}(M)\kappa^* + \mathbf{w} + O[\delta(\|\mathbf{w}\|_2 + \|M\|_2)] \end{aligned}$$

$$\begin{aligned}\mathcal{P}^{(2)}(\mathbf{y}) &\triangleq \frac{1}{n} X^2 \mathbf{y} - \mathcal{P}^{(0)}(\mathbf{y}) = \\ \mathcal{D}(M)(\boldsymbol{\phi}^* - 1) + \mathcal{D}(\boldsymbol{\kappa}^*) \mathbf{w} + O[\delta(\|\mathbf{w}\|_2 + \|M\|_2)] ,\end{aligned}$$

provided $n \geq C_\eta k d / \delta^2$.

Lemma 6 shows that $\mathcal{A}' X^\top$ and $\mathcal{P}^{(t,\cdot)}$ are all concentrated around their expectations with no more than $O(C_\eta k^2 d)$ samples. To finish our construction of the moment estimation sequence, we need to bound the deviation of G and H from their expectation G^* and H^* . This is done in the following lemma.

Lemma 7. *Suppose $\mathbb{P}(\mathbf{x})$ is τ -MIP. Then in Algorithm 1, for any $j \in \{1, \dots, d\}$,*

$$\|G - G^*\|_\infty \leq \delta, \quad \|H - H^*\|_\infty \leq \delta ,$$

provided

$$n \geq C_\eta \frac{1}{\tau} \left(1 + \frac{1}{\tau} \sqrt{\|\boldsymbol{\kappa}^*\|_\infty^2 + \|\boldsymbol{\phi}^* - 3\|_\infty^2}\right) / \delta^2 .$$

Lemma 7 shows that $G \approx G^*$ as long as $n \geq O(1/\tau^2)$. Since G is the solution of Eq. (7), it requires $\mathbb{P}(\mathbf{x})$ must be τ -MIP with $\tau > 0$. When $\tau = 0$, for example on binary Bernoulli distribution, we must use the construction in subsection 3.1 instead. As the non-MIP moment estimation sequence doesn't invoke the inversion of moment matrices, the sampling complexity will not depend on $O(1/\tau)$.

We are now ready to give the condition of Eq. (10) being true.

Lemma 8. *Under the same settings of Theorem 2, with probability at least $1 - \eta$, Eq. (10) holds true provided*

$$n \geq C_\eta (p + 1)^2 / \delta^2 \max\{p/\tau^2, k^2 d\}$$

where $p \triangleq \max\{1, \|\boldsymbol{\kappa}^*\|_\infty, \|\boldsymbol{\phi}^* - 3\|_\infty, \|\boldsymbol{\phi}^* - 1\|_\infty\}$.

Lemma 8 shows that the sampling complexity to guarantee Eq. (10) is bounded by $O(k^2 d)$ or $O(1/\tau^2)$, depending on which one dominates. The proof of Lemma 8 consists of two steps. First we replace each operator or matrix with its expectation plus a small perturbation given in Lemma 6 and Lemma 7. Then Lemma 8 follows after simplification.

Theorem 2 is obtained by combining Lemma 8 and Theorem 3.

5 Experiments

We verify our theory on synthetic datasets in subsection 5.1 and demonstrate several applications of the SLM on real-world datasets in subsection 5.2. We implement Algorithm 1 in Python. We fuse the notation 'SLM' to present our solver of the second order linear model in this section. We choose the fastFM Bayer [2016] toolbox as the baseline solver of a special case of the SLM based

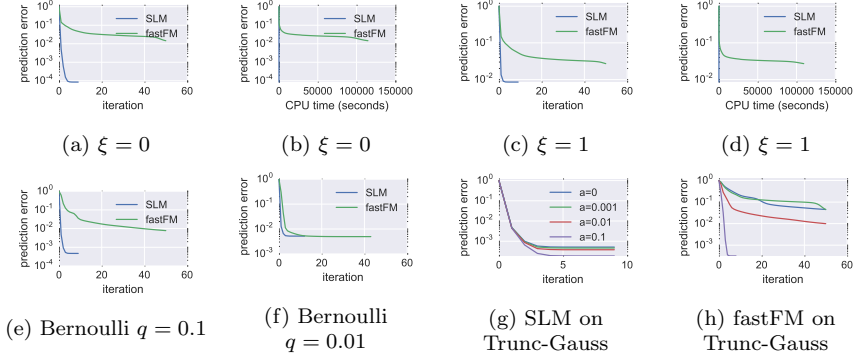


Figure 1: Convergence curve. (a)-(d): truncated Gaussian distribution with low-rank M^* ; (e)-(h): $\mathcal{D}(M^*) = \mathbf{0}$.

Table 1: Rating Prediction MSE and Relation Prediction AUC

	Movielens100k	Movielens1M	Flixster-Rating	Epinions	Flixter-Relation	OMIM
SLM	0.870	0.818	0.784	0.919	0.645	0.721
fastFM	0.838	0.764	0.779	0.894	0.626	0.684
SVM/SVR	1.25	1.13	1.01	0.917	0.708	0.748

on gradient descent heuristic. Please note that both fastFM and libFM only allow $M^* = VV^\top - \mathcal{D}(VV^\top)$ for some matrix $V \in \mathbb{R}^{d \times k}$. FastFM is shown to be faster and more robust than libfm Rendle [2012] on real-world problems. The SVR and SVM are the baseline linear models in regression tasks and in classification tasks respectively. Our computer has 32 GB memory and a 64 bit, 8 core CPU. Our implementation and datasets will be released on our website after publication.

5.1 Synthetic Datasets

In this subsection, we verify the global convergence of Algorithm 1 on MIP and non-MIP distributions. We will show that the gradient descent heuristic cannot work well when the distribution is skewed.

In the following experiments, the dimension $d = 1000$ and the rank $k = 10$. Since non-MIP distributions require M^* to be diagonal-free, we generate M^* under two different low-rank models. For MIP distributions, we randomly generate $U \in \mathbb{R}^{d \times k}$ such that $U^\top U = I$. Then we produce $M^* = UU^\top$. Please note that our model allows symmetric but non-PSD M^* but due to space limitations we only demonstrate the PSD case in this work. For non-MIP distributions, we generate $\bar{M}^* = UU^\top$ similarly and take $M^* = \bar{M}^* - \mathcal{D}(\bar{M}^*)$. The \mathbf{w}^* is randomly sampled from $\mathcal{N}(\mathbf{0}, 1/d)$. The noise term ξ is sampled from $\xi \cdot \mathcal{N}(\mathbf{0}, I)$ where ξ is the noise level in set $\{0, 1\}$. All synthetic experiments are repeated 10 trials in order to report the average performance. In each trial,

we randomly sample $30kd$ training instances and 10,000 testing instances. The running time is measured by the number of iterations and CPU time in seconds separately. Please note that fastFM is written in highly optimized C code for sparse features therefore the CPU time may not be a fair index. In fastFM we set the regularizer to be zero to avoid the convex bias. The estimation accuracy is measured by the normalized mean squared error $[\mathbb{E}(y_{\text{pred}} - y_{\text{true}})^2]/\mathbb{E}(y_{\text{true}}^2)$. We terminate the experiment after 50 iterations or when the training error decreases less than 10^{-8} between two consecutive iterations.

It is important to emphasize that we don't use the zero mean and unit variance oracle in our experiment. Therefore the recovery error is lower bounded by $\Omega(\max\{1, \kappa, \phi\}/\sqrt{n})$ since this is the statistical error level of moment estimation. In the SLM if we use the above moment oracle, we can achieve exactly zero recovery error. Please check our journal version for this experiment. In the following we say a method achieving zero recovery error if the statistical error level is achieved.

MIP Distributions In this experiment we sample \mathbf{x} from truncated Gaussian distribution which is MIP. To sample \mathbf{x} , we first generate a Gaussian random number \hat{x} then truncate $x = \min\{\hat{x}, a\}$ where a is the truncation level. The convergence curves of $a = 0$ are reported in Figure 1 (a)-(d). FastFM consumes significantly more CPU time. This is mostly because fastFM is not optimized for dense features. In real-world datasets where features are sparse, fastFM is always faster than our Python implementation of SLM. For a fair comparison we prefer the number of iterations as computation cost. It is not surprising that fastFM cannot achieve zero error on noise-free datasets in Figure 1 (a) and (c) because the conventional FM model cannot recover non-zero diagonal elements of M^* . SLM converges linearly and achieve zero error on noise-free datasets. In noisy datasets SLM is robust to noise.

Non-MIP Distributions We turn to verify our theory on non-MIP distributions where $\mathcal{D}(M^*) = 0$. Note that the non-MIP moment estimation sequence can be applied to MIP distributions as long as M^* is diagonal-free. As we constrain ourselves on PSD matrices (although not necessary), we expect the conventional FM model achieving zero recovery error under the non-MIP setting. To this end we always set the noise level $\xi = 0$ in the following experiments. However we will shortly show that fastFM, due to its gradient descent nature, is unable to achieve zero recovery error on skewed distributions.

The first example we considered is the binary Bernoulli distribution where $\mathbb{P}(x = 1) = q$ otherwise $x = 0$. We choose $q = \{0.1, 0.01\}$. The convergence curves are reported in Figure 1 (e) and (f). SLM converges fast in both (e) and (f). Note that when the distribution becomes skewed, the convergence rate depends on $\|\kappa\|_\infty$. Therefore it is expected to achieve a relative large prediction error when $p = 0.01$. When $p = 0.1$ in Figure 1 (e). The convergence rate of fastFM is again much slower than SLM. Indeed it seems fastFM is unable to converge globally after long iterations. When $p = 0.01$ in (e), fastFM seems to

converge to the same solution as SLM. It is actually because $p = 0.01$ is too skewed such that both solvers cannot achieve small recovery error due to the moment estimation error.

As we analyzed in Section 4, the failure of the gradient descent heuristic in the SLM is because the gradient is bias by $O(\|\kappa\|_\infty)$. We expect the convergence of fastFM being worse when the skewness of the distribution is larger. To verify this, we report the convergence curves of SLM and fastFM on truncated Gaussian with $a = \{0, 10^{-3}, 0.01, 0.1\}$ in Figure 1 (g) and (h). As we expected, when $a \rightarrow 0$, the skewness becomes larger and the fastFM converges worse. When $a = 0$, fastFM is unable to find the global optimal solution at all. In contrast, SLM always converges globally and linearly under any a .

5.2 Real-World Datasets

In this subsection, we demonstrate several applications of the SLM on real-word datasets. Please be advised that in this introductory work we didn't attempt to argue the superiority of the SLM on these datasets. It really depends on whether the problem at hand satisfies the second order linear model assumption and how well the features are engineered. When the problem is linearly separable, the SLM is very likely to perform worse than the linear model due to its $O(k^2d)$ sampling complexity when $k > 1$.

We consider two real-world problems which are popular in recommendation system: the Rating Prediction problem and the Relation Prediction problem. In each experiment, we randomly split 20% instances as testing set and use five fold cross-validation to tune parameters. All experiments are repeated 10 trials and then the averaged performance on the testing set is evaluated. For FM and SLM, we tune the rank k in set $\{1, 2, 4, 8, 12, 16\}$. The ℓ_2 -norm regularizers are tuned in set $\{10, 1, 0.1, \dots\}$. For SVR/SVM, the parameter C is tuned from 10^{-4} to 10^4 .

Rating Prediction In our rating prediction tasks, a user-item rating matrix is partially observed. The goal is to recover the missing rating scores which minimizes the mean squared error (MSE). In addition, we are given user feature and item feature that present the characteristics of the user and the item. Following previous works, we model the rating score y as an unknown function of user feature \mathbf{x}_u and item feature \mathbf{x}_c . As a standard technique, we extend the feature with one-hot encoding. We collect the following three datasets for the rating prediction tasks: *Movielens100k*, *Movielens1M*, *Flixster-Rating*. The dataset description can be found in Appendix F. The MSE scores of SLM and baseline methods are summarized in Table 1.

Relation Prediction The goal of relation prediction is to predict whether any pair of two instances have relationship. In each dataset, we take all the observed positive relation as the positive samples. We randomly sample negative samples from the unobserved relations, which are 5 times amounts of the positive

samples. We are given features that present the characteristics of instances. We use the same feature encoding pipeline as in the rating prediction problem. We collect the following three datasets for the relation prediction tasks: *Epinions*, *Flixster-Relation*, *OMIM*. The dataset description can be found in Appendix F. The AUC scores of SLM and baseline methods are summarized in Table 1.

From Table 1, SLM and fastFM are better in rating prediction but not as good as SVM in relation prediction. FastFM is the best model on all three rating prediction datasets. This might be because the PSD regularization of FM model better fits the rating prediction problem. SLM achieves similar performance on most datasets as FM model because it is a generalized version of FM. In general there is no model always superior than other models on all datasets.

6 Conclusion

We develop a nonconvex gradient-free learning framework, which we call the moment-estimation-sequence method, to analyze the convergence rate and the sampling complexity of the SLM on general sub-gaussian distributions. The proposed method can learn the SLM with low computational cost. The sampling complexity of our estimation is $O(C_\eta k^2 d)$ which is nearly optimal up to a factor $C_\eta k$. The proposed learning framework, moment-estimation-sequence method, can be applied to other kinds of learning problems where the gradient descent heuristic cannot work well or even fail to converge.

References

Immanuel Bayer. fastFM: A Library for Factorization Machines. *Journal of Machine Learning Research*, 17(184):1–5, 2016.

Mathieu Blondel, Masakazu Ishihata, Akinori Fujino, and Naonori Ueda. Polynomial Networks and Factorization Machines: New Insights and Efficient Training Algorithms. In *Proceedings of The 33rd International Conference on Machine Learning*, pages 850–858, 2016.

T. Tony Cai and Anru Zhang. ROP: Matrix recovery via rank-one projections. *The Annals of Statistics*, 43(1):102–138, 2015.

E. Candes, Y. Eldar, T. Strohmer, and V. Voroninski. Phase Retrieval via Matrix Completion. *SIAM Journal on Imaging Sciences*, 6(1):199–225, 2013.

E. J. Candes and Y. Plan. Tight Oracle Inequalities for Low-Rank Matrix Recovery From a Minimal Number of Noisy Random Measurements. *IEEE Transactions on Information Theory*, 57(4):2342–2359, 2011.

Thomas Hofmann, Bernhard Schölkopf, and Alexander J. Smola. Kernel methods in machine learning. *The Annals of Statistics*, 36(3):1171–1220, 2008.

Prateek Jain and Inderjit S. Dhillon. Provable inductive matrix completion. *arXiv preprint arXiv:1306.0626*, 2013.

V. Koltchinskii. *Oracle Inequalities in Empirical Risk Minimization and Sparse Recovery Problems*, volume 2033. Springer, 2011.

Richard Kueng, Holger Rauhut, and Ulrich Terstiege. Low rank matrix recovery from rank one measurements. *Applied and Computational Harmonic Analysis*, 42(1): 88–116, 2017.

Ming Lin and Jieping Ye. A Non-convex One-Pass Framework for Generalized Factorization Machine and Rank-One Matrix Sensing. In *NIPS*, 2016.

Yurii Nesterov. *Introductory Lectures on Convex Optimization: A Basic Course*, volume 87. Springer, 2004.

Steffen Rendle. Factorization machines. In *IEEE 10th International Conference On Data Mining*, pages 995–1000, 2010.

Steffen Rendle. Factorization Machines with libFM. *ACM Trans. Intell. Syst. Technol.*, 3(3):57:1–57:22, 2012.

Roman Vershynin. *High-Dimensional Probability: An Introduction with Applications in Data Science*. 2017.

Mark Rudelson and Roman Vershynin. Hanson-Wright inequality and sub-gaussian concentration. *Electronic Communications in Probability*, 18, 2013.

Terence Tao. *Topics in Random Matrix Theory*, volume 132. Amer Mathematical Society, 2012.

Joel A. Tropp. Convex Recovery of a Structured Signal from Independent Random Linear Measurements. In *Sampling Theory, a Renaissance*, Applied and Numerical Harmonic Analysis, pages 67–101. Springer International Publishing, 2015.

A. Vedaldi and A. Zisserman. Efficient Additive Kernels via Explicit Feature Maps. *IEEE Transactions on Pattern Analysis and Machine Intelligence*, 34(3):480 –492, 2012.

Tuo Zhao, Zhaoran Wang, and Han Liu. A Nonconvex Optimization Framework for Low Rank Matrix Estimation. In *NIPS*, pages 559–567. 2015.

A Preliminary

The ψ_2 -Orlicz norm of a random sub-gaussian variable z is defined by

$$\|z\|_{\psi_2} \triangleq \inf\{t > 0 : \mathbb{E} \exp(z^2/t^2) \leq c\}$$

where $c > 0$ is a constant. For a random sub-gaussian vector $\mathbf{z} \in \mathbb{R}^n$, its ψ_2 -Orlicz norm is

$$\|\mathbf{z}\|_{\psi_2} \triangleq \sup_{\mathbf{x} \in S^{n-1}} \|\langle \mathbf{z}, \mathbf{x} \rangle\|_{\psi_2}$$

where S^{n-1} is the unit sphere.

The following theorem gives the matrix Bernstein's inequality Roman Vershynin [2017].

Theorem 9 (Matrix Bernstein's inequality). *Let X_1, \dots, X_N be independent, mean zero $d \times n$ random matrices with $d \geq n$ and $\|X_i\|_2 \leq B$. Denote*

$$\sigma^2 \triangleq \max\left\{\left\|\sum_{i=1}^N \mathbb{E} X_i X_i^\top\right\|_2, \left\|\sum_{i=1}^N \mathbb{E} X_i^\top X_i\right\|_2\right\}.$$

Then for any $t \geq 0$, we have

$$\mathbb{P}\left(\left\|\sum_{i=1}^N X_i\right\|_2 \geq t\right) \leq 2d \exp\left[-c \min\left(\frac{t^2}{\sigma^2}, \frac{t}{B}\right)\right].$$

where c is a universal constant. Equivalently, with probability at least $1 - \eta$,

$$\left\|\sum_{i=1}^N X_i\right\|_2 \leq c \max\left\{B \log(2d/\eta), \sigma \sqrt{\log(2d/\eta)}\right\}.$$

When $\mathbb{E} X_i \neq \mathbf{0}$, replacing X_i with $X_i - \mathbb{E} X_i$ the inequality still holds true.

The following Hanson-Wright inequality for sub-gaussian variables is given in Rudelson and Vershynin [2013].

Theorem 10 (Sub-gaussian Hanson-Wright inequality). *Let $\mathbf{x} = [x_1, \dots, x_d] \in \mathbb{R}^d$ be a random vector with independent, mean zero, sub-gaussian coordinates. Then given a fixed $d \times d$ matrix M , for any $t \geq 0$,*

$$\mathbb{P}\left\{|\mathbf{x}^\top A \mathbf{x} - \mathbb{E} \mathbf{x}^\top A \mathbf{x}| \geq t\right\} \leq 2 \exp\left[-c \min\left(\frac{t^2}{B^4 \|A\|_F^2}, \frac{t}{B^2 \|A\|_2}\right)\right],$$

where $B = \max_i \|X_i\|_{\psi_2}$ and c is a universal positive constant. Equivalently, with probability at least $1 - \eta$,

$$|\mathbf{x}^\top A \mathbf{x} - \mathbb{E} \mathbf{x}^\top A \mathbf{x}| \leq c \max\{B^2 \|A\|_2 \log(2/\eta), B^2 \|A\|_F \sqrt{\log(2/\eta)}\}.$$

The next lemma estimates the covering number of low-rank matrices Candes and Plan [2011].

Lemma 11 (Covering number of low-rank matrices). *Let $S = \{M \in \mathbb{R}^{d \times d} : \text{rank}(M) \leq k, \|M\|_F \leq c\}$ be the set of rank- k matrices with unit Frobenius norm. Then there is an ϵ -net cover of S , denoted as $\bar{S}(\epsilon)$, such that*

$$|\bar{S}(\epsilon)| \leq (9c/\epsilon)^{(2d+1)k}.$$

Note that the original lemma in Candes and Plan [2011] bounds $\|M\|_F = 1$ but in the above lemma we slightly relax to $\|M\|_F \leq c$. The proof is nearly the same as the original one.

Truncation trick As Bernstein's inequality requires boundness of the random variable, we use the truncation trick in order to apply it on unbounded random matrices. First we condition on the tail distribution of random matrices to bound the norm of a fixed random matrix. Then we take union bound over all n random matrices in the summation. The union bound will result in an extra $O[\log(n)]$ penalty in the sampling complexity which can be absorbed into C_η or c_η . Please check [Tao, 2012] for more details.

B Proof of Theorem 5

Define $p_1 = 2 + \|\phi^* - 3\|_\infty$. Recall that

$$\frac{1}{n} \mathcal{A}' \mathcal{A}(M) = \frac{1}{n} \sum_{i=1}^n \mathbf{x}^{(i)} \mathbf{x}^{(i)\top} M \mathbf{x}^{(i)} \mathbf{x}^{(i)\top}.$$

Denote

$$\begin{aligned} Z_i &\triangleq \mathbf{x}^{(i)} \mathbf{x}^{(i)\top} M \mathbf{x}^{(i)} \mathbf{x}^{(i)\top} \\ \mathbb{E} Z_i &= 2M + \text{tr}(M)I + \mathcal{D}(\phi^* - 3)\mathcal{D}(M). \end{aligned}$$

In order to apply matrix Bernstein's inequality, we have

$$\begin{aligned} \|Z_i\|_2 &= \|\mathbf{x}^{(i)} \mathbf{x}^{(i)\top} M \mathbf{x}^{(i)} \mathbf{x}^{(i)\top}\|_2 \\ &\leq \|\mathbf{x}^{(i)\top} M \mathbf{x}^{(i)}\| \|\mathbf{x}^{(i)} \mathbf{x}^{(i)\top}\|_2 \\ &\leq \|\mathbf{x}^{(i)\top} M \mathbf{x}^{(i)}\| \|\mathbf{x}^{(i)}\|_2^2 \\ &\leq c_\eta \|M\|_F \|\mathbf{x}^{(i)}\|_2^2 \\ &\leq c_\eta \|M\|_F d. \end{aligned}$$

And

$$\begin{aligned} \|\mathbb{E} Z_i\|_2 &= \|2M + \text{tr}(M)I + \mathcal{D}(\phi^* - 3)\mathcal{D}(M)\|_2 \\ &\leq 2\|M\|_2 + |\text{tr}(M)| + \|\phi^* - 3\|_\infty \|M\|_2 \\ &\leq (2 + \|\phi^* - 3\|_\infty) \|M\|_2 + |\text{tr}(M)| \\ &\leq p_1 \|M\|_2 + |\text{tr}(M)|. \end{aligned}$$

And

$$\begin{aligned} \|\mathbb{E} Z_i Z_i^\top\|_2 &= \|\mathbb{E} \mathbf{x}^{(i)} \mathbf{x}^{(i)\top} M \mathbf{x}^{(i)} \mathbf{x}^{(i)\top} \mathbf{x}^{(i)} \mathbf{x}^{(i)\top} M \mathbf{x}^{(i)} \mathbf{x}^{(i)\top}\|_2 \\ &\leq c_\eta d \|\mathbb{E} \mathbf{x}^{(i)} \mathbf{x}^{(i)\top} M \mathbf{x}^{(i)} \mathbf{x}^{(i)\top} M \mathbf{x}^{(i)} \mathbf{x}^{(i)\top}\|_2 \\ &\leq c_\eta d \|\mathbb{E} \mathbf{x}^{(i)} \mathbf{x}^{(i)\top}\|_2 \|\mathbf{x}^{(i)\top} M \mathbf{x}^{(i)}\|^2 \\ &\leq c_\eta d \|\mathbb{E} \mathbf{x}^{(i)} \mathbf{x}^{(i)\top}\|_2 \|M\|_F^2 \\ &\leq c_\eta d \|M\|_F^2. \end{aligned}$$

And

$$\begin{aligned} \|(\mathbb{E} Z_i)(\mathbb{E} Z_i)^\top\|_2 &\leq \|\mathbb{E} Z_i\|_2^2 \\ &\leq [p_1 \|M\|_2 + |\text{tr}(M)|]^2 \end{aligned}$$

$$\leq 2p_1\|M\|_2 + 2|\text{tr}(M)| .$$

Therefore we get

$$\begin{aligned}\|Z_i - \mathbb{E}Z_i\|_2 &\leq \|Z_i\|_2 + \|\mathbb{E}Z_i\|_2 \\ &\leq c_\eta\|M\|_F d + p_1\|M\|_2 + |\text{tr}(M)| .\end{aligned}$$

And

$$\begin{aligned}\text{Var1} &\triangleq \|(Z_i - \mathbb{E}Z_i)(Z_i - \mathbb{E}Z_i)^\top\|_2 \\ &\leq \|Z_i Z_i^\top\|_2 + \|(\mathbb{E}Z_i)(\mathbb{E}Z_i)^\top\|_2 \\ &\leq c_\eta d\|M\|_F^2 + 2p_1\|M\|_2 + 2|\text{tr}(M)| .\end{aligned}$$

Suppose that

$$\begin{aligned}d\|M\|_F^2 &\geq 2p_1\|M\|_2 + 2|\text{tr}(M)| \\ \Leftrightarrow d &\geq (2p_1\|M\|_2 + 2|\text{tr}(M)|) \frac{1}{\|M\|_F^2} \\ \Leftrightarrow d &\geq 2p_1 + 2|\text{tr}(M)| \frac{1}{\|M\|_F^2} \\ \Leftrightarrow d &\geq 2p_1 + 2\sqrt{k} .\end{aligned}$$

The we get

$$\begin{aligned}\|Z_i - \mathbb{E}Z_i\|_2 &\leq c_\eta\|M\|_F d \\ \text{Var1} &\leq c_\eta d\|M\|_F^2 .\end{aligned}$$

Then according to matrix Bernstein's inequality,

$$\begin{aligned}\left\| \frac{1}{n} \sum_{i=1}^n Z_i - \mathbb{E}Z_i \right\|_2 &= c_\eta \max \left\{ \frac{1}{n} \|M\|_F d, \frac{1}{\sqrt{n}} \sqrt{d\|M\|_F^2} \right\} \\ &\leq c_\eta \frac{1}{\sqrt{n}} \sqrt{d\|M\|_F} \\ &\leq c_\eta \sqrt{\frac{kd}{n}} \|M\|_2 .\end{aligned}$$

provided

$$\begin{aligned}\frac{1}{n} \|M\|_F d &\leq \frac{1}{\sqrt{n}} \sqrt{d\|M\|_F^2} \\ \Leftrightarrow n &\geq d .\end{aligned}$$

C Proof of Lemma 6

Proof. To prove $\frac{1}{n}\mathcal{A}'(X^\top \mathbf{w})$,

$$\frac{1}{n}\mathcal{A}'(X^\top \mathbf{w}) = \frac{1}{n} \sum_{i=1}^n \mathbf{x}^{(i)} \mathbf{x}^{(i)\top} \mathbf{w} \mathbf{x}^{(i)} \mathbf{x}^{(i)\top} .$$

Similar to Theorem 5, just replacing $\mathcal{A}(M)$ with \mathbf{w} , then with probability at last $1 - \eta$,

$$\left\| \frac{1}{n} \mathcal{A}'(X^\top \mathbf{w}) - \mathcal{D}(\boldsymbol{\kappa}^*) \mathbf{w} \right\|_2 \leq C_\eta \sqrt{d/n} \|\mathbf{w}\|_2 .$$

Therefore let

$$n \geq C_\eta d / \delta^2 .$$

We have

$$\left\| \frac{1}{n} \mathcal{A}'(X^\top \mathbf{w}) - \mathcal{D}(\boldsymbol{\kappa}^*) \mathbf{w} \right\|_2 \leq \delta \|\mathbf{w}\|_2 .$$

To prove $\mathcal{P}^{(0)}(\mathbf{y})$,

$$\mathcal{P}^{(0)}(\mathbf{y}) = \frac{1}{n} \sum_{i=1}^n \mathbf{x}^{(i)\top} \mathbf{w} + \frac{1}{n} \sum_{i=1}^n \mathbf{x}^{(i)\top} M \mathbf{x}^{(i)} .$$

Since \mathbf{x} is coordinate sub-gaussian, any $i \in \{1, \dots, d\}$, with probability at least $1 - \eta$,

$$\|\mathbf{x}^{(i)\top} \mathbf{w}\|_2 \leq c\sqrt{d} \|\mathbf{w}\|_2 \log(n/\eta) .$$

Then we have

$$\left\| \frac{1}{n} \sum_{i=1}^n \mathbf{x}^{(i)\top} \mathbf{w} - 0 \right\|_2 \leq C\sqrt{d} \|\mathbf{w}\|_2 \log(n/\eta) / \sqrt{n} .$$

From Hanson-Wright inequality,

$$\begin{aligned} \left\| \frac{1}{n} \sum_{i=1}^n \mathbf{x}^{(i)\top} M \mathbf{x}^{(i)} - \text{tr}(M) \right\|_2 &\leq C \|M\|_F \log(1/\eta) \\ &\leq C \sigma_1 \sqrt{k/n} \log(1/\eta) . \end{aligned}$$

Therefore

$$\begin{aligned} \mathcal{P}^{(0)}(\mathbf{y}) &= \text{tr}(M) + O[(\sqrt{d} \|\mathbf{w}\|_2 + \|M\|_2 \sqrt{k}) / \sqrt{n} \log(n/\eta)] \\ &= \text{tr}(M) + O[C_\eta (\sqrt{d} \|\mathbf{w}\|_2 + \|M\|_2 \sqrt{k}) / \sqrt{n}] \\ &= \text{tr}(M) + O[C_\eta (\|\mathbf{w}\|_2 + \|M\|_2 \sqrt{k}) \sqrt{d/n}] . \end{aligned}$$

Let

$$n \geq C_\eta k d / \delta^2 .$$

We have

$$\mathcal{P}^{(0)}(\mathbf{y}) = \text{tr}(M) + O[\delta(\|\mathbf{w}\|_2 + \|M\|_2)] .$$

To prove $\mathcal{P}^{(1)}(\mathbf{y})$,

$$\mathcal{P}^{(1)}(\mathbf{y}) = \frac{1}{n} \sum_{i=1}^n \mathbf{x}^{(i)} \mathbf{x}^{(i)\top} \mathbf{w} + \frac{1}{n} \sum_{i=1}^n \mathbf{x}^{(i)} \mathbf{x}^{(i)\top} M \mathbf{x}^{(i)} .$$

From covariance concentration inequality,

$$\begin{aligned} \left\| \frac{1}{n} \sum_{i=1}^n \mathbf{x}^{(i)} \mathbf{x}^{(i)\top} \mathbf{w} - \mathbf{w} \right\|_2 &\leq c \sqrt{d/n} \|\mathbf{w}\|_2 \log(d/\eta) \\ &\leq C_\eta \sqrt{d/n} \|\mathbf{w}\|_2 . \end{aligned}$$

To bound the second term in $\mathcal{P}^{(1)}(\mathbf{y})$,

Apply Hanson-Wright inequality again,

$$\begin{aligned} \|\mathbf{x}^{(i)} \mathbf{x}^{(i)\top} M \mathbf{x}^{(i)}\|_2 &\leq \|\mathbf{x}^{(i)}\|_2 \|\mathbf{x}^{(i)\top} M \mathbf{x}^{(i)}\|_2 \\ &\leq c[\|M\|_F + \text{tr}(M)] \sqrt{d} \log^2(nd/\eta) \\ &\leq C_\eta k \|M\|_2 \sqrt{d} . \end{aligned}$$

By matrix Chernoff's inequality, choose $n \geq c_\eta k^2 d / \delta^2$,

$$\begin{aligned} \left\| \frac{1}{n} \sum_{i=1}^n \mathbf{x}^{(i)} \mathbf{x}^{(i)\top} M \mathbf{x}^{(i)} - \mathcal{D}(M) \boldsymbol{\kappa}^* \right\|_2 &\leq C_\eta k \|M\|_2 \sqrt{d/n} \\ &\leq \delta \|M\|_2 . \end{aligned}$$

Therefore we have

$$\mathcal{P}^{(1)}(\mathbf{y}) = \mathbf{w} + \mathcal{D}(M) \boldsymbol{\kappa}^* + O[\delta(\|\mathbf{w}\|_2 + \|M\|_2)] .$$

To bound $\mathcal{P}^{(2)}(\mathbf{y})$, first note that

$$\begin{aligned} \mathcal{P}^{(2)}(\mathbf{y}) &= \frac{1}{n} \sum_{i=1}^n \mathbf{x}^{(i)2} \mathbf{x}^{(i)\top} \mathbf{w} + \frac{1}{n} \sum_{i=1}^n \mathbf{x}^{(i)2} \mathbf{x}^{(i)\top} M \mathbf{x}^{(i)} - P^{(0)}(\mathbf{y}) \\ &= \frac{1}{n} \sum_{i=1}^n \mathcal{D}(\mathbf{x}^{(i)} \mathbf{x}^{(i)\top} \mathbf{w} \mathbf{x}^{(i)}) + \frac{1}{n} \sum_{i=1}^n \mathcal{D}(\mathbf{x}^{(i)} \mathbf{x}^{(i)\top} M \mathbf{x}^{(i)} \mathbf{x}^{(i)\top}) - P^{(0)}(\mathbf{y}) . \end{aligned}$$

Then similarly,

$$\left\| \frac{1}{n} \sum_{i=1}^n \mathbf{x}^{(i)2} \mathbf{x}^{(i)\top} \mathbf{w} - \mathcal{D}(\boldsymbol{\kappa}^*) \mathbf{w} \right\|_2 \leq C_\eta \sqrt{d/n} \|\mathbf{w}\|_2$$

$$\left\| \frac{1}{n} \sum_{i=1}^n \mathbf{x}^{(i)2} \mathbf{x}^{(i)\top} M \mathbf{x}^{(i)} - \text{tr}(M) - \mathcal{D}(M)(\phi^* - 1) \right\|_2 \leq k \|M\|_2 \sqrt{d/n} .$$

The last inequality is because Theorem 5. Combine all together, choose $n \geq c_\eta k^2 d$,

$$\begin{aligned} \mathcal{P}^{(2)}(\mathbf{y}) &= \mathcal{D}(\boldsymbol{\kappa}^*) \mathbf{w} + \mathcal{D}(M)(\phi^* - 1) + O(C_\eta \sqrt{d/n} \|\mathbf{w}\|_2) \\ &\quad + O(\sigma_1 k \sqrt{d/n}) + O[C_\eta(\|\mathbf{w}\|_2 + k \|M\|_2) \sqrt{d/n}] \\ &= \mathcal{D}(\boldsymbol{\kappa}^*) \mathbf{w} + \mathcal{D}(M)(\phi^* - 1) + O[C_\eta(\|\mathbf{w}\|_2 + \|M\|_2) k \sqrt{d/n}] \\ &= \mathcal{D}(\boldsymbol{\kappa}^*) \mathbf{w} + \mathcal{D}(M)(\phi^* - 1) + O[\delta(\|\mathbf{w}\|_2 + \|M\|_2)] . \end{aligned}$$

□

D Proof of Lemma 7

The next lemma bounds the estimation accuracy of κ^*, ϕ^* . It directly follows sub-gaussian concentration inequality and union bound.

Lemma 12. *Given n i.i.d. sampled $\mathbf{x}^{(i)}$, $i \in \{1, \dots, n\}$. With a probability at least $1 - \eta$,*

$$\begin{aligned}\|\kappa - \kappa^*\|_\infty &\leq C_\eta / \sqrt{n} \\ \|\phi - \phi^*\|_\infty &\leq C_\eta / \sqrt{n}\end{aligned}$$

provided $n \geq C_\eta d$.

Denote G^* as G in Eq. (7) but computed with κ^*, ϕ^* . The next lemma bounds $\|G_{j,:} - G_{j,:}^*\|_2$ for any $j \in \{1, \dots, d\}$.

Proof. Denote $\mathbf{g} = G_j$, $\mathbf{g}^* = G_j^*$, $\kappa = \kappa_j$, $\phi = \phi_j$,

$$\begin{aligned}A &= \begin{bmatrix} 1 & \kappa_j \\ \kappa_j & \phi_j - 1 \end{bmatrix}, \quad \mathbf{b} = \begin{bmatrix} \kappa_j \\ \phi_j - 3 \end{bmatrix} \\ A^* &= \begin{bmatrix} 1 & \kappa_j^* \\ \kappa_j^* & \phi_j^* - 1 \end{bmatrix}, \quad \mathbf{b}^* = \begin{bmatrix} \kappa_j^* \\ \phi_j^* - 3 \end{bmatrix}.\end{aligned}$$

Then $\mathbf{g} = A^{-1}\mathbf{b}$, $\mathbf{g}^* = A^{*-1}\mathbf{b}^*$. Since $\mathbb{P}(\mathbf{x})$ is τ -MIP, $\|A^{*-1}\|_2 \leq 1/\tau$. From Lemma 12,

$$\begin{aligned}\|A - A^*\|_2 &\leq C \log(d/\eta) / \sqrt{n} \\ \|\mathbf{b} - \mathbf{b}^*\|_2 &\leq C \log(d/\eta) / \sqrt{n}.\end{aligned}$$

Define $\Delta_A \triangleq A - A^*$, $\Delta_b \triangleq \mathbf{b} - \mathbf{b}^*$, $\Delta_g \triangleq \mathbf{g} - \mathbf{g}^*$,

$$\begin{aligned}A\mathbf{g} &= \mathbf{b} \\ \Leftrightarrow (A^* + \Delta_A)(\mathbf{g}^* + \Delta_g) &= \mathbf{b}^* + \Delta_b \\ \Leftrightarrow A^*\Delta_g + \Delta_A\mathbf{g}^* + \Delta_A\Delta_g &= \Delta_b \\ \Leftrightarrow (A^* + \Delta_A)\Delta_g &= \Delta_b - \Delta_A\mathbf{g}^* \\ \Rightarrow \|(A^* + \Delta_A)\Delta_g\|_2 &= \|\Delta_b - \Delta_A\mathbf{g}^*\|_2 \\ \Rightarrow \|(A^* + \Delta_A)\Delta_g\|_2 &\leq \|\Delta_b\|_2 + \|\Delta_A\mathbf{g}^*\|_2 \\ \Rightarrow \|(A^* + \Delta_A)\Delta_g\|_2 &\leq C \log(d/\eta) / \sqrt{n} + C \log(d/\eta) / \sqrt{n} \|\mathbf{g}^*\|_2 \\ \Rightarrow \|(A^* + \Delta_A)\Delta_g\|_2 &\leq C \log(d/\eta) / \sqrt{n} (1 + \|\mathbf{g}^*\|_2) \\ \Rightarrow \|(A^* + \Delta_A)\Delta_g\|_2 &\leq C \log(d/\eta) / \sqrt{n} (1 + \frac{1}{\tau} \|\mathbf{b}^*\|_2) \\ \Rightarrow \|(A^* + \Delta_A)\Delta_g\|_2 &\leq C \log(d/\eta) / \sqrt{n} (1 + \frac{1}{\tau} \sqrt{\kappa^2 + (\phi - 3)^2}) \\ \Rightarrow [\tau - C \log(d/\eta) / \sqrt{n}] \|\Delta_g\|_2 &\leq C \log(d/\eta) / \sqrt{n} (1 + \frac{1}{\tau} \sqrt{\kappa^2 + (\phi - 3)^2}).\end{aligned}$$

When

$$\begin{aligned}\tau - C \log(d/\eta) / \sqrt{n} &\geq \frac{1}{2} \tau \\ \Leftrightarrow n &\geq 4C^2 \log^2(d/\eta) / \tau^2,\end{aligned}$$

we have

$$\|\Delta_g\|_2 \leq \frac{2C}{\tau\sqrt{n}} \log(d/\eta) \left(1 + \frac{1}{\tau} \sqrt{\kappa^2 + (\phi - 3)^2}\right).$$

Since Δ_g is a vector of dimension 2, its ℓ_2 -norm bound also controls its ℓ_∞ -norm bound up to constant. Choose

$$n \geq C_\eta \frac{1}{\tau} \left(1 + \frac{1}{\tau} \sqrt{\kappa^2 + (\phi - 3)^2}\right) / \delta^2.$$

We have

$$\|\Delta_g\|_\infty \leq \delta.$$

The proof of H is similar. \square

E Proof of Lemma 8

Proof. To abbreviate the notation, we omit $\hat{\mathbf{y}}^{(t)} - \mathbf{y}^{(t)}$ and superscript t in the following proof. Denote $\mathcal{H}^* = \mathbb{E}\mathcal{H}$ and the expectation of other operators similarly. By construction in Algorithm 2,

$$\begin{aligned} \mathcal{M} &\triangleq \mathcal{H} - \frac{1}{2}\mathcal{D}(G_1 \circ \mathcal{P}^{(1)}) - \frac{1}{2}\mathcal{D}(G_2 \circ \mathcal{P}^{(2)}) \\ &= \mathcal{H}^* + O[\delta(\alpha_{t-1} + \beta_{t-1})] \\ &\quad - \frac{1}{2}\mathcal{D}(G_1^* \circ \mathcal{P}^{*(1)}) - \frac{1}{2}\mathcal{D}(G_2^* \circ \mathcal{P}^{*(2)}) \\ &\quad + O[\|G - G^*\|_\infty (\|\mathcal{P}^{*(1)}\|_2 + \|\mathcal{P}^{*(2)}\|_2)] \\ &\quad + O[\|G - G^*\|_\infty \delta(\alpha_{t-1} + \beta_{t-1})] \\ &= M^{(t)} - M^* + O[\delta(\alpha_{t-1} + \beta_{t-1})] \\ &\quad + O[\delta(\|\mathcal{P}^{*(1)}\|_2 + \|\mathcal{P}^{*(2)}\|_2)] \\ &\quad + O[\delta^2(\alpha_{t-1} + \beta_{t-1})] \\ &= M^{(t)} - M^* + O[\delta(\alpha_{t-1} + \beta_{t-1})] \\ &\quad + O[\delta(\|\mathcal{P}^{*(1)}\|_2 + \|\mathcal{P}^{*(2)}\|_2)] \\ &= M^{(t)} - M^* + O[\delta(\alpha_{t-1} + \beta_{t-1})] \\ &\quad + O[\delta(\alpha_{t-1}\|\kappa^*\|_\infty + \beta_{t-1}) \\ &\quad + \alpha_{t-1}\|\phi^* - 1\|_\infty + \beta_{t-1}\|\kappa^*\|_\infty] \\ &= M^{(t)} - M^* + O[\delta(\alpha_{t-1} + \beta_{t-1})] + O[\delta p(\alpha_{t-1} + \beta_{t-1})] \\ &= M^{(t)} - M^* + O[\delta(p+1)(\alpha_{t-1} + \beta_{t-1})]. \end{aligned}$$

The above requires

$$\begin{aligned} n &\geq \max\{C_\eta \frac{1}{\tau} (1 + \frac{1}{\tau} \sqrt{\kappa^2 + (\phi - 3)^2}) / \delta^2, C_\eta k^2 d\} \\ &= \max\{C_\eta p(\tau\delta)^{-2}, C_\eta k^2 d\}. \end{aligned}$$

Replace $\delta(p+1)$ with δ , the proof is completed.

To bound $\mathcal{W}^{(t)}(\hat{\mathbf{y}}^{(t)} - \mathbf{y}^{(t)})$, similarly we have

$$\begin{aligned}
\mathcal{W} &= G_1 \circ \mathcal{P}^{(1)} + G_2 \circ \mathcal{P}^{(2)} \\
&= G_1^* \circ \mathcal{P}^{*(1)} + G_2^* \circ \mathcal{P}^{*(2)} \\
&\quad + O[\|G - G^*\|_\infty \delta(\alpha_{t-1} + \beta_{t-1})] \\
&\quad + O[\|G - G^*\|_\infty (\|\mathcal{P}^{*(1)}\|_2 + \|\mathcal{P}^{*(2)}\|_2)] \\
&= \mathbf{w}^{(t-1)} - \mathbf{w}^* + O[\delta^2(\alpha_{t-1} + \beta_{t-1})] \\
&\quad + O[\delta p(\alpha_{t-1} + \beta_{t-1})] \\
&= \mathbf{w}^{(t-1)} - \mathbf{w}^* + O[\delta(p+1)(\alpha_{t-1} + \beta_{t-1})].
\end{aligned}$$

□

F Datasets

*Movielens100k*¹ is a benchmark rating prediction dataset publicly available online. It consists of observed 100,000 ratings (1-5) from 943 users on 1,682 movies. For each user, we construct a 825-dimensional features by binary encoding with the information of the user's age, gender, occupation and zip-code. And for each movie, 19-dimensional features are built with binary encoding from its genre information. The features of each rating here are the concatenation of the associated user's and item's features, which are of 844 dimensions.

*Movielens1M*² is a superset of Movielens100k. This dataset has 1,000,209 ratings (1-5) on 3,952 movies made by 6,040 users. We extract 3,648-dimensional features for each user and 18-dimensional features for each movie. Then the features of each rating are the concatenation of the associated user's and movie's features, which are of 3,666 dimensions.

*Flixster*³ is a movie review dataset with user linkage network. We randomly sample a subset of 309,870 ratings by 10,468 users on 6,843 movies. The dataset is endowed with an undirected social network of all users. For each user, we encode its binary social connection with others as the user feature, which turns out to be a vector of 10,468 dimension. Note that there are no features designed for movies in this dataset.

*Epinions*⁴ contains the directed social link relations and users' ratings on a set of items. By random sampling from the original dataset, we obtain 93,863 positive social links that are generated by 9,309 users. In addition, each user has the ratings (1-5) on 7,695 items. We use the users' ratings as their own features, which are of 7,695 dimensions. Then the features of each user-user interaction is the concatenation of the two associated users' features, which are of 15,390 dimensions.

The *Flixster* used in the rating prediction task can be served as relation prediction benchmark. We do a random sampling from the original dataset to build a subset that contains 55,304 positive users' undirected links from 10,468 users. Besides, each user has the ratings (1-5) on 6,843 movies. We encode the users' ratings as their features,

¹<http://grouplens.org/datasets/movielens/100k/>

²<http://grouplens.org/datasets/movielens/1m/>

³<http://www.cs.ubc.ca/~jamalim/datasets/>

⁴<http://www.cs.ubc.ca/~jamalim/datasets/>

which are of 6,843 dimensions. Then the features of each user-user interaction are the concatenation of the two associated users features, which are of 13,686 dimensions.

OMIM is a human gene-disease interaction data collected by Jain and Dhillon [2013]. The dataset consists of 3,954 positive observed relations formed by 3,209 diseases and 12,331 genes. We represent each disease by tf-idf features of 16,592 dimensions describing each disease. We represent each gene with 29,811-dimensional features. They are concatenated by 3 type of features, which are concatenation of the 12,331-dimensional similarity scores in the HumanNet gene interaction network, 12,944-dimensional gene-phenotype associations from 8 other species and 4,536-dimensional microarray expression data. Then the features of each gene-disease interaction are the concatenation of the associated gene features and disease features, which are of 46,403 dimensions.